scientific reports



OPEN

A finite element with statistical analysis study to investigate the electrical performance of composite insulators under water droplet impact

Lyamine Ouchen¹, Khaled Belhouchet²[□], Abdelhafid Bayadi¹, Abderrahim Zemmit², Abdelhakim Idir², Yayehyirad Ayalew Awoke³[□], Enas Ali⁴, Sherif. S. M. Ghoneim⁵ & Ahmed B. Abou Sharaf^{6,7}

Composite insulators demonstrate superior electrical performance in contrast to standard insulators. Nevertheless, the deterioration of composite insulator and the challenges in identifying defects are the primary drawbacks of these insulators. This study investigates the effect of water droplets on the electrical behavior of composite insulators, which are widely used in high-voltage applications. Using COMSOL software, a Finite Element Model (FEM) was developed to simulate the electric field distribution on the surface of a composite insulator in the presence of water droplets. The results indicate that the existence of water droplets increases the electric field intensity by approximately 33.33% when the number of droplets increases from two to six. The simulations also reveal that water droplets significantly increase the electric field's intensity, which affects the electric field and potential distribution on the insulator's surface. Furthermore, the conductivity of water droplets was found to have a negligible impact on the electric field distribution along the insulator. To systematically evaluate the influence of various factors, Response Surface Methodology (RSM) was employed in combination with Analysis of Variance (ANOVA) to analyze the interactions between water droplet number, pollution, and applied voltage. The statistical analysis demonstrated that the maximum electric field intensity increased by nearly 38.3% as water droplet conductivity rose from low to high levels. RSM was used to generate a second-order polynomial model that describes the relationship between these factors and the electrical performance of the insulator, allowing for the identification of significant trends and interactions. The findings provide valuable insights for the design and development of composite insulators that are more resilient to environmental factors, enhancing their overall electrical performance.

Keywords ANOVA, Composite insulator, Electric field, FEM, Water droplet

High-voltage insulators are critical components in ensuring the safety and reliability of electrical power transmission and distribution networks. Their performance directly influences the stability and longevity of these systems, particularly under challenging environmental conditions. Over the years, significant progress has been made in the development of insulators, transitioning from traditional porcelain and glass materials to advanced composite insulators. Early studies focused on porcelain insulators, which provided adequate

¹Department of Electrical Engineering, Faculty of Technology, Ferhat Abbas University, Setif − 1, Setif 19000, Algeria. ²Department of Electrical Engineering, Electrical Engineering Laboratory (LGE), University of M'Sila, M'Sila 28000, Algeria. ³3Department of Electrical and Computer Engineering, Debre Markos Institute of Technology, Debre Markos University, P. BOX 269, Debre Markos, Ethiopia. ⁴University Centre for Research and Development, Chandigarh University, Mohali 140413, Punjab, India. ⁵Department of Electrical Engineering, College of Engineering, Taif University, Taif 21944, Saudi Arabia. ⁶Ministry of Higher Education & Scientific Research, Industrial Technical Institute in Mataria, Cairo 11718, Egypt. ⁷Centre for Research Impact & Outcome, Chitkara University Institute of Engineering and Technology, Chitkara University, Rajpura 140401, Punjab, India. [™]email: khaled.belhouchet@univ-msila.dz; yayehyirad_ayalew@dmu.edu.et

mechanical and electrical performance but were prone to issues such as brittleness and heavy weight^{1,2}. In the 1990s, the adoption of polymer-based composite insulators marked a breakthrough, driven by their lightweight nature, superior mechanical properties, and resistance to environmental stresses³. However, these advancements introduced new challenges, particularly in predicting long-term performance and understanding the interaction between external factors and the material properties of composite insulators.

Composite insulators, which are increasingly replacing traditional porcelain and glass insulators, offer several advantages. Their lightweight, high mechanical strength, superior hydrophobicity, and enhanced resistance to environmental stressors make them a cost-effective and efficient solution in high-voltage applications⁴. However, their sensitivity to electric fields and external conditions, particularly the presence of water droplets, poses a significant challenge. Water droplets on the surface of composite insulators can lead to reduced electrical performance, increased risk of partial discharges, and ultimately, flashovers. Research dating back to the early 2000s has highlighted the role of water droplets in distorting electric fields, creating localized areas of high stress that accelerate material degradation⁵. Subsequent experimental and computational studies have investigated various scenarios, including the impact of droplet size, conductivity, and distribution on electrical performance, offering valuable insights into these phenomena^{6,7}. In addition, advances in simulation techniques, such as Finite Element Modeling (FEM), have enhanced our understanding of electric field behavior on insulator surfaces under wet conditions. However, early models often lacked the precision and validation necessary to account for real-world conditions8. Recent efforts have focused on refining these models and incorporating statistical analysis methods, such as to evaluate complex interactions among multiple variables, paving the way for more reliable insulator designs^{9,10}. The distribution of the electric field along the insulator surface is a key factor influencing the occurrence of discharges. Non-uniform electric fields create regions of high stress that can lead to corona discharges, dry band arcing, and surface erosion, ultimately causing insulation failure¹¹. Water droplets on the surface further distort the electric field, increasing the likelihood of flashover. This phenomenon is particularly prominent in silicone rubber insulators, where the flashover mechanism is linked to the behavior of water droplets under the influence of an electric field.

Previous studies have employed experimental and simulation techniques to assess the degradation of insulator surfaces due to discharge activities and dry band arcing 12-17. However, the accuracy of current simulations remains limited by oversimplified models and inadequate validation of stress distributions 18-20. This research aims to address these gaps by employing advanced Finite Element Method (FEM) simulations using COMSOL Multiphysics to enhance the understanding of electric field distribution around composite insulators under water droplet impact.

This study addresses the critical challenge of understanding the influence of water droplets on the electrical performance of composite insulators, a key factor in ensuring the reliability of High-voltage (HV) power systems. The novelty of this work lies in its detailed analysis of electric field intensification caused by water droplets and its implications for surface flashovers and material degradation. By combining advanced Finite Element Method (FEM) simulations using COMSOL Multiphysics with statistical analysis through analysis of variance (ANOVA), this research provides a comprehensive understanding of localized electric field distortions. These findings fill a critical gap in the literature and offer practical methodologies to optimize the design and improve the reliability of composite insulators in challenging environmental conditions.

Simulation setup and methodology

This study employs finite element simulations to analyze the electrical performance of composite insulators subjected to water droplet impact. The simulations, conducted using various instruments and computational tools, offer a comprehensive analysis of the insulator behavior under varying droplet parameters. This section outlines the simulation setup, the instrumentation involved, and the computational techniques employed.

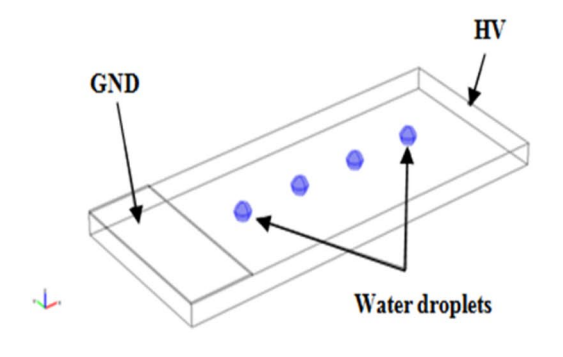
The simulations were performed using COMSOL Multiphysics, a powerful software platform widely used for simulating coupled physical phenomena.

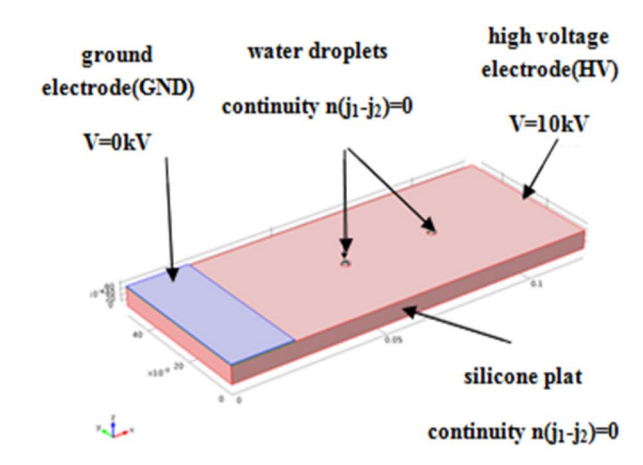
The simulation setup, shown in Fig. 1, features a silicone plate $(120 \times 50 \times 6 \text{ mm}^3)$ with two steel electrodes arranged in a tip-plane configuration. This setup is designed to analyze the electric field distribution and the interaction between water droplets and the insulator surface. Table 1 details the material properties used in the simulations, including the permittivity and conductivity of the silicone insulator. Accurate modeling of these parameters is crucial for reflecting the electrical behavior of the composite insulator under various voltage conditions and for understanding how different droplet distributions and material properties impact insulator performance in high-voltage environments.

Droplet distribution and modeling

In this study, water droplets are systematically distributed across the surface of the composite insulator to analyze their impact on electrical performance. The study examines three scenarios, where the number of droplets; 2, 4, and 6; varies to ensure comprehensive coverage of the insulator's surface, as outlined in Table 2. The High-Voltage (HV) side is selected for analysis due to its critical role in electric field distribution. The droplets are modeled with radii of 1.5 mm, 2.5 mm, and 3.5 mm across the scenarios. Additionally, the droplets have a hemispherical shape, and their dielectric constants and electrical conductivities are adjusted to low, medium, and high levels (10 μ S, 30 μ S, and 50 μ S) to thoroughly evaluate how these variations influence the insulator's performance under different applied potentials of 10 kV, 20 kV, and 30 kV.

The simulation setup, shown in Fig. 1, features a silicone plate $(120 \times 50 \times 6 \text{ mm}^3)$ with two steel electrodes arranged in a tip-plane configuration. This setup is designed to analyze the electric field distribution and the interaction between water droplets and the insulator surface. Table 2 details the material properties used in the simulations, including the permittivity and conductivity of the silicone insulator. Accurate modeling of these parameters is crucial for reflecting the electrical behavior of the composite insulator under various voltage





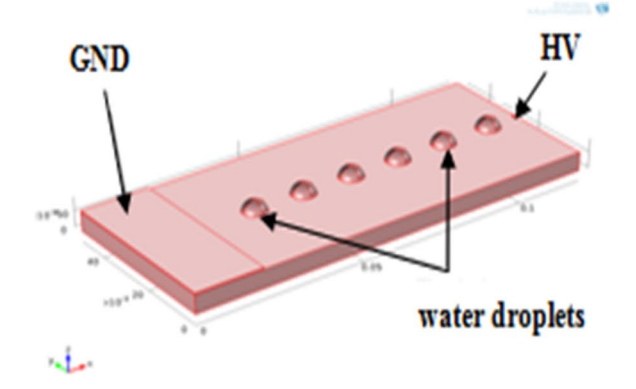


Fig. 1. Simulation Setup and Water Droplet Distribution on Composite Insulator.

Type of material	Relative Electric permittivity, ε_r	Electric Conductivity, σ(S/cm)
Silicone	4,3	10^{-14}
Steel electrodes	1000	5.9×10^{7}
Water drops	81	$(9.4 - 18.6 - 27.8) \times 10^7$
Air	1	10^{-15}

Table 1. Electrical properties of materials used in FEM simulations^{21,22}.

Studied scenarios	Scenario 1	Scenario 2	Scenario 3
Number	2	4	6
Conductivity (µS)	10/30/50	10/30/50	10/30/50
Radius (mm)	1.5	2.5	3.5
Voltage (kV)	10/20/30	10/20/30	10/20/30

Table 2. Parameters and scenarios analyzed for droplet distribution on insulators.

conditions and for understanding how different droplet distributions and material properties impact insulator performance in high-voltage environments.

Experimental design

In this work, the Design of Experiments (DoE) approach was employed using Response Surface Methodology (RSM) to systematically investigate the impact of key parameters on the electrical performance of composite insulators subjected to water droplet impact. The main factors considered in the design include droplet size, droplet conductivity, droplet distribution, and applied voltage. The approach is well-suited for exploring the interaction effects between multiple factors, while minimizing the number of simulations required. It incorporates both factorial and star points to ensure that a broad range of factor combinations are covered, and allows for the estimation of quadratic effects. This design is particularly useful in capturing the nonlinear relationships between the variables and the output responses, such as flashover voltage and electric field distribution.

To model the system, the data obtained from the simulations were analyzed using RSM, which fits a secondorder polynomial model to the experimental results. The polynomial model provides a clear representation of how each factor, as well as their interactions, affects the output responses. Additionally, Analysis of Variance (ANOVA) was used to assess the statistical significance of the factors and interactions, ensuring that the model is both accurate and reliable.

The levels of the factors were selected based on preliminary studies and the operational conditions of composite insulators in high-voltage applications.

Instruments for data acquisition and validation

In this study, a combination of advanced software tools and instruments was employed to ensure the accuracy and reliability of the simulation results. COMSOL Multiphysics 5.6 served as the primary tool for conducting the finite element simulations, enabling the solution of electrostatic equations and visualization of key parameters such as electric potential and field intensity. The software's advanced visualization capabilities were essential for analyzing the spatial distribution of the electric field around water droplets and assessing the risk of flashover. For statistical analysis and validation of the simulation results, Minitab was utilized. This software facilitated the implementation of Response Surface Methodology and Analysis of Variance to evaluate the effects of varying droplet parameters and applied voltages on the insulator's performance. Minitab's robust statistical tools enabled the identification of significant trends and provided a rigorous approach to ensure the validity of the findings. Additionally, a computational cluster was used to run parallel simulations with varying mesh sizes and droplet configurations, optimizing computational efficiency while maintaining the accuracy of results, especially for simulations with fine mesh configurations. These tools collectively contributed to a comprehensive and reliable analysis of the electrical performance of composite insulators under water droplet impact.

Numerical approach for electrical performance analysis

The numerical approach allows for the accurate modeling of the electric field behavior in the presence of water droplets, considering their dielectric properties and distribution across the insulator surface. The Finite Element Method (FEM) is employed to discretize the physical domain of the insulator into smaller, manageable elements. This method provides a flexible and precise means of solving complex electrostatic problems, particularly in cases involving heterogeneous materials and irregular geometries. In the context of this study, the FEM allows for the analysis of the composite insulator's behavior under various loading conditions, including different water droplet sizes, conductivity levels, and applied voltages.

Governing equations and simulation framework for composite insulators

This section provides an overview of the governing equations and simulation framework used in our finite element study of composite insulators subjected to water droplet impacts. We utilized COMSOL Multiphysics to simulate two scenarios: a baseline clean insulator model and a more complex model with water droplets on the insulator's surface.

Electric field (E) was determined according to Eq. (1):¹⁰.

$$E = -\nabla V \tag{1}$$

• Electric potential (V) was calculated according to Eq. (2):

$$\nabla \cdot (\sigma \nabla V) + \frac{\partial}{\partial t} \nabla \cdot (\epsilon \nabla V) = 0$$
 (2)

• For the case of no charge density ($\rho = 0$), as defined in Eq. (3):

$$\nabla^2 V = 0 \tag{3}$$

• In Cartesian coordinates, the equation is expressed as in Eq. (4):

$$\frac{\partial^2 V}{\partial x^2} + \frac{\partial^2 V}{\partial y^2} + \frac{\partial^2 V}{\partial z^2} = 0 \tag{4}$$

• The function for isotropic permittivity is given by Eq. (5):

$$F(V) = \frac{1}{2} \iiint \epsilon |\nabla * V|^2 dv$$
 (5)

Finally, including conductivity, as shown in Eq. (6):

$$F(V) = \frac{1}{2} \iiint (\sigma + j\omega \epsilon) |\nabla * V|^2 dv$$
 (6)

Where ω is angular frequency.

These equations form the foundation of the finite element model, which was employed to simulate the insulator's electrical behavior accurately. The model's results were further validated through statistical analysis,

Mesh type	Number of Elements	Number of iterations	Computing time [s]	Error
Extra fine	229,624	351	69	9.95*10 ⁻⁷
Fine	95,913	121	10	1.12*10-7
Normal	15,126	50	0.86	4.6*10-6
Coarse	8865	35	0.59	8.3*10-5
Extra coarse	1831	26	0.28	5.68*10-4

Table 3. Comparison results for different mesh types.

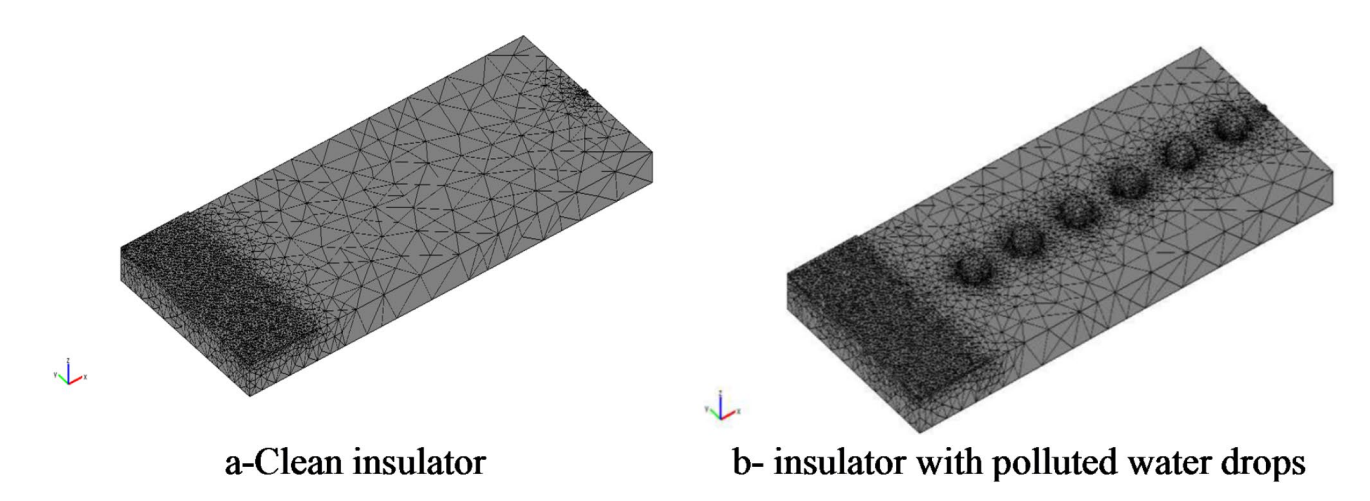


Fig. 2. Mesh geometry under clean and polluted conditions.

which involved running multiple simulations with varying parameters to identify significant trends and ensure the reliability of our findings.

3.1 Impact of mesh size on simulation accuracy and computational efficiency

The effect of mesh size on simulation accuracy and computational efficiency was assessed using the clean insulator model, analyzing five mesh types: extra fine, fine, normal, coarse, and extra coarse, as detailed in Table 3. The extra fine mesh provided the highest accuracy with the lowest error but was computationally demanding, taking 69 s for 351 iterations. On the other hand, the extra coarse mesh, while significantly faster at 0.28 s for 26 iterations, resulted in the highest error.

The normal mesh was chosen for the entire simulation as it offered a balanced trade-off between accuracy and computational efficiency. It delivered reliable results while optimizing resource use. Figure 2 shows the meshing configurations for both clean and polluted conditions, with each scenario using an appropriately sized element to ensure effective analysis.

Results and discussion

The analysis of the electrical performance of composite insulators under the influence of water droplets was conducted using a finite element model. The simulations focused on the distribution of electric potential in the insulator's surface under varying conditions of water droplet presence. This section presents the results derived from these simulations, which illustrate the impact of water droplets on the electric field distribution across the insulator surface.

Figure 3 shows the electric potential distribution on a composite insulator's surface under different water droplet conditions and applied voltages. Without water droplets (Fig. 3a), the potential distribution was uniform, but with two droplets (Fig. 3b), the potential concentrated locally, distorting the electric field. The effect became more pronounced with four droplets (Fig. 3c), leading to more complex potential patterns. Six aligned droplets (Fig. 3d) further amplified these distortions, creating several high-potential areas. These results demonstrated that even small surface contamination significantly increased electric field intensity, raising the risk of surface flashover and insulation degradation. A correlation analysis was performed to explore the relationships between the number of droplets, applied voltage, and electric potential distribution. The analysis revealed a strong positive correlation between the number of droplets and the degree of electric field distortion. As the number of droplets increased, the potential distribution became increasingly non-uniform, as shown in Fig. 3a and d. Additionally, a strong correlation was observed between the applied voltage and the size of high-potential regions. Higher voltages (20 kV in Figs. 3b and 30 kV in Fig. 3c and d) resulted in larger and more intense high-potential areas, indicating that increased voltage amplifies the electric stress on the insulator surface.

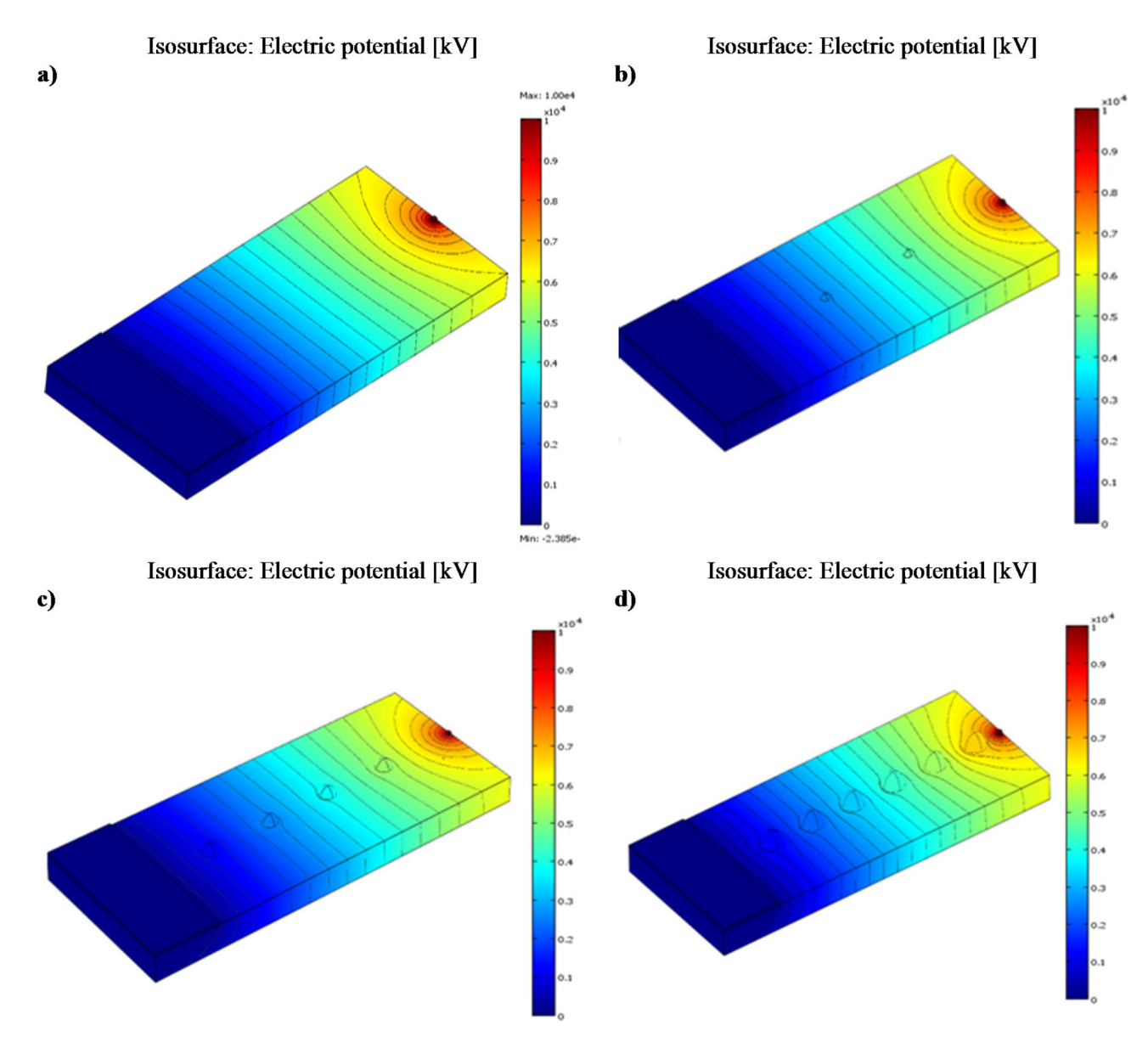


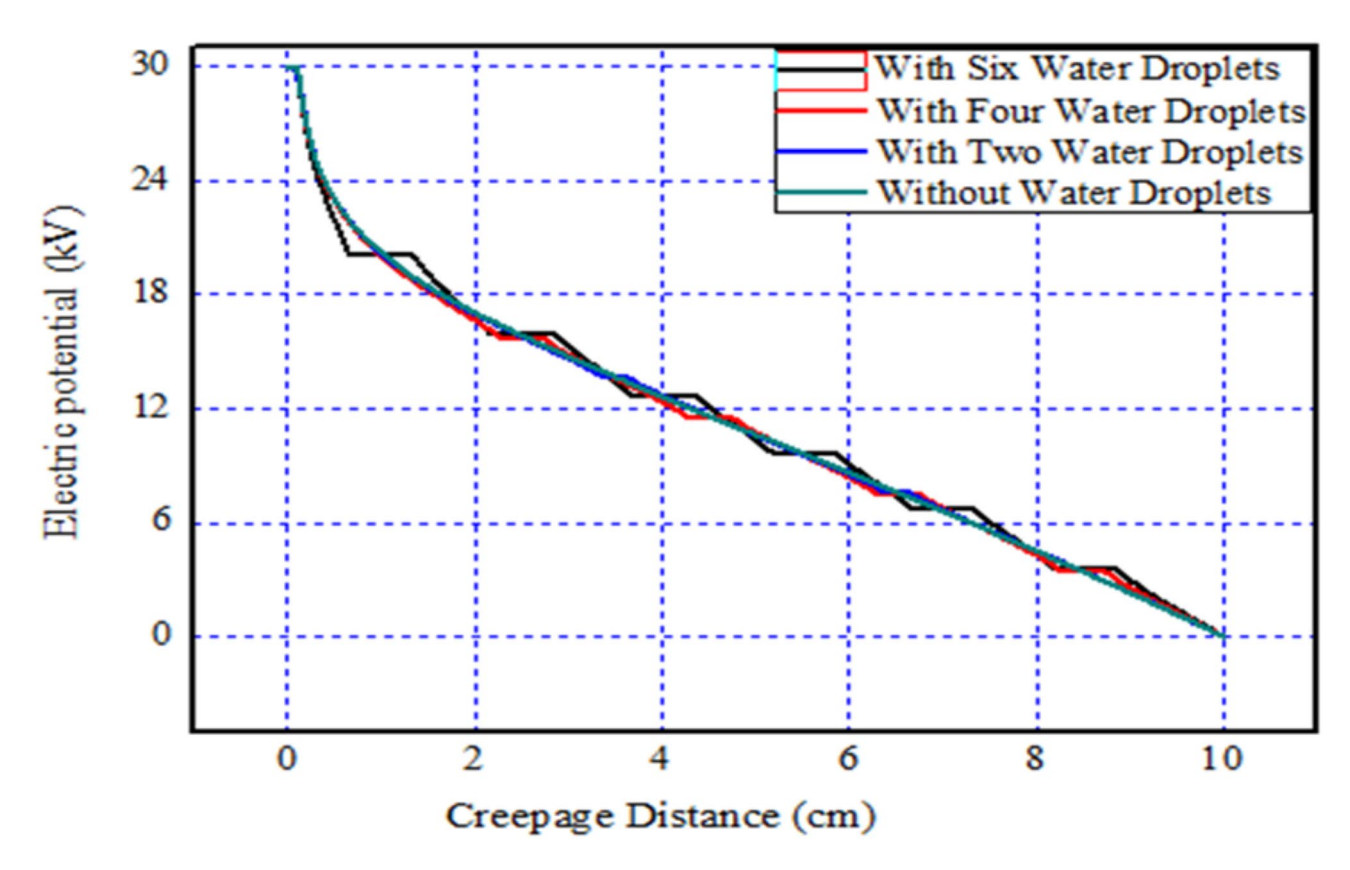
Fig. 3. Distribution of Equipotential lines on composite insulators under varying water droplet conditions.

The applied voltages for these conditions were $10\,\mathrm{kV}$ (a), $20\,\mathrm{kV}$ (b), and $30\,\mathrm{kV}$ (c, d), and the results illustrated the variation of potential along the creepage distance. The electric potential was highest near the high-volder end and decreased towards the grounded end. As the applied voltage increased from $10\,\mathrm{kV}$ to $30\,\mathrm{kV}$, the high-potential area expanded, indicating increased electric stress along the insulator surface.

These findings from the correlation analysis emphasize the critical role of water droplet coverage and applied voltage in affecting potential gradients. The interplay between these factors significantly influences the likelihood of flashover, highlighting the need for effective insulation design and maintenance in high-voltage applications.

Figure 4 demonstrates the impact of varying numbers of water droplets on the electrical potential distribution along the creepage distance of a composite insulator under a 30 kV applied voltage. In a dry condition, the potential decreases uniformly, serving as a baseline. The introduction of two droplets causes minor deviations, with slight dips and peaks in the potential gradient. With four droplets, these fluctuations become more pronounced, indicating increased perturbation. Finally, with six droplets, the potential distribution exhibits significant deviations, highlighting the cumulative disruptive effect of multiple droplets on the otherwise linear potential gradient.

The study reveals that the overall trend in electrical potential along the creepage distance decreases consistently under high voltage conditions. However, the introduction of water droplets causes localized disturbances in this potential distribution, with the magnitude of these disturbances increasing as the number of droplets grows. These deviations suggest that water droplets influence the electric field along the insulator's surface, potentially leading to concentrated areas of electrical stress. Although the potential distribution remains generally linear, the presence of droplets poses a risk of electrical discharges, particularly at these localized points. This highlights



 $\textbf{Fig. 4.} \ \ \text{Electrical potential distribution along the creepage distance of a composite insulator under a 30 kV applied voltage. } \\$

the importance of understanding such variations for designing composite insulators capable of withstanding environmental challenges, thus ensuring their long-term reliability and effectiveness in practical applications.

Figure 5 provides an analysis of how varying numbers of water droplets impact the electric field distribution along a composite insulator's creepage distance under a high voltage of 30 kV. In dry conditions without droplets, the electric field starts at about 80 kV/cm near the electrode and rapidly decreases, stabilizing around 10 kV/cm beyond 10 cm, which is typical and minimizes discharge risks.

However, the presence of two water droplets introduces localized disruptions, creating minor peaks in the electric field around 20 kV/cm. With four droplets, these peaks become more pronounced, reaching up to 30 kV/cm, showing a cumulative effect where each droplet increasingly distorts the field. The most significant disruption occurs with six droplets, where the field peaks at approximately 60 kV/cm at multiple points along the creepage distance, nearly doubling the field strength compared to fewer droplets.

These findings suggest that the accumulation of water droplets leads to concentrated areas of electrical stress, increasing the risk of surface or partial discharges. These discharges can degrade the insulator material, compromising its insulation strength and leading to potential failure. Notably, the electric field remains elevated even beyond 10 cm of creepage distance, indicating that the influence of droplets extends farther along the surface than initially expected.

This analysis underscores the critical importance of accounting for environmental factors like water droplet formation when designing and maintaining composite insulators, particularly in high-voltage applications. Understanding how droplets interact with the electric field helps engineers anticipate potential failure points and incorporate design improvements or protective measures to enhance the insulator's durability and reliability in moisture-prone environments.

The simulations assessing the impact of varying numbers of water droplets (with a uniform radius of $3.5\,\mathrm{mm}$) on the electric field distribution under a constant applied voltage of $30\,\mathrm{kV}$ show significant trends. As depicted in Fig. 6, increasing the droplet count from 2 to 6 results in a higher concentration of equipotential lines around the droplets, indicating stronger localized electric fields. From Fig. 7, it is evident that the electric field along the creepage distance increases sharply near the droplet locations, with a maximum field value of approximately $80\,\mathrm{kV/cm}$ for six droplets, which represents an approximate 33.33% increase compared to the maximum field for two droplets, at $60\,\mathrm{kV/cm}$.

Figure 8 further illustrates this trend, showing that the maximum electric field rises by about 16.7% when increasing from two to four droplets and by another 21.4% from four to six droplets. These results highlight the pronounced impact of water droplet accumulation on electric field intensification, which may exacerbate stress on composite insulators.

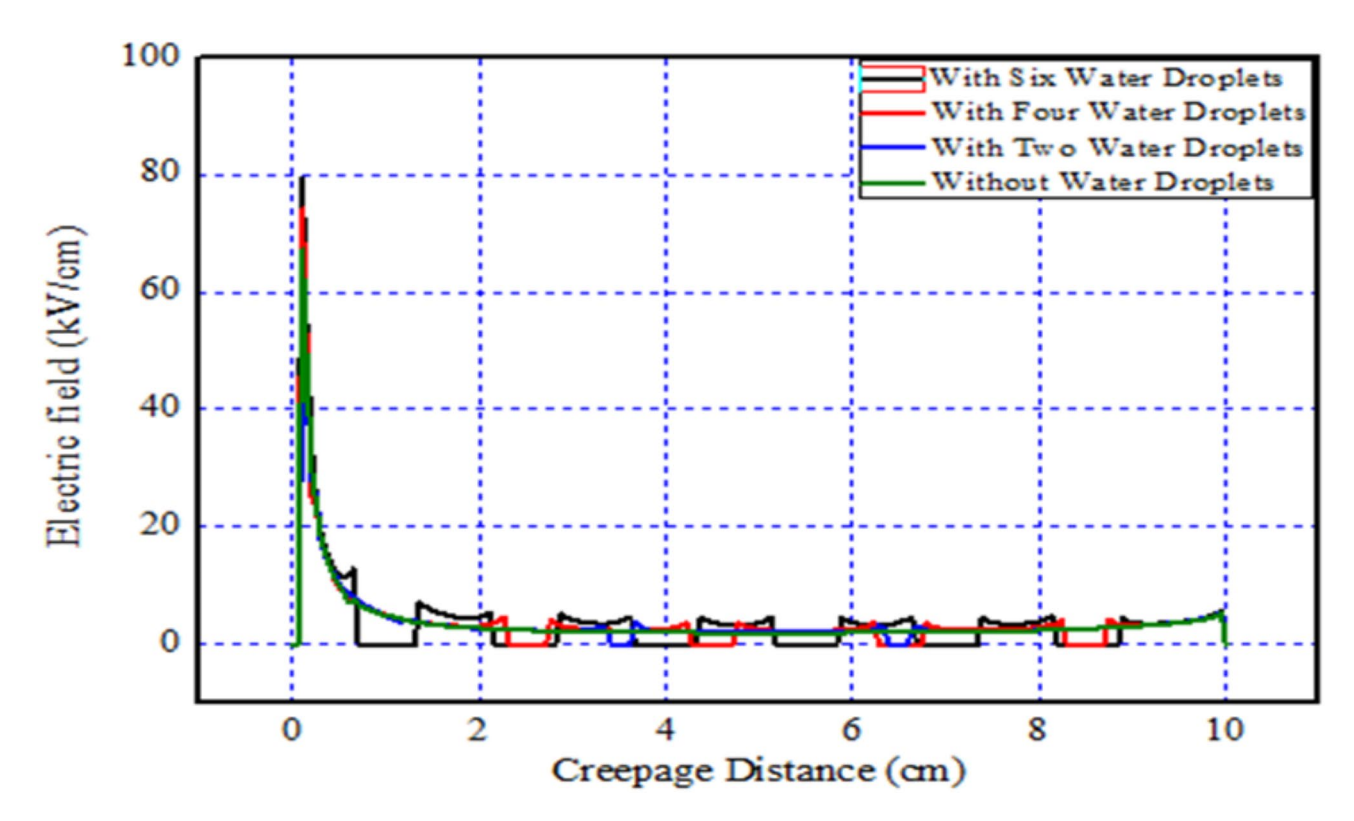


Fig. 5. Detailed analysis of the electric field distribution along the creepage distance of a composite insulator under a high applied voltage of 30 kV.

To better understand the relationship between the maximum electric field intensity (Emax) and the number of water droplets (n), regression analysis was conducted for the data presented in Fig. 8. For this graph, the relationship was found to be linear and was represented using a first-degree polynomial equation as shown in Eq. (7):

$$y = a + b.x \tag{7}$$

Where the variable y expresses the maximum electric field intensity value and the variable x expresses the number of water droplets, and thus the previous equation becomes as follows:

$$E_{max} = a + b.n \tag{8}$$

Where:

n: is the number of water droplets,

 E_{max} : maximum electric field intensity value,

b: slope = 463,600

a: intercept = 5,115,930

The variation in the electric field norm along the creepage distance for composite insulators under different applied voltages: 10 kV, 20 kV, and 30 kV is illustrated in Fig. 9. The electric field intensity sharply peaks near the beginning of the creepage path and gradually diminishes, with smaller peaks recurring at intervals along the distance. The magnitude of the electric field increases with higher applied voltage, with the 30 kV curve consistently higher than the 20 kV and 10 kV curves. The analysis indicates that the electric field is most intense at the initial points of the creepage path and is influenced significantly by the applied voltage.

Under water droplet conditions, the initial sections of the insulator, referring to the areas closest to the high-voltage electrode and corresponding to the start of the creepage distance, exhibit significantly higher electric field intensities. This is evidenced by the sharp peak observed at the beginning of the curve in Fig. 9. The high field intensity in these sections is attributed to the needle-plate electrode configuration used in the simulation, where the sharp geometry of the needle concentrates the electric field near the electrode tip. As the distance from the electrode increases, the electric field intensity gradually decreases along the creepage path, following the characteristic non-uniform field distribution of needle-type geometries. These surface areas, being more susceptible to elevated electric field stress, may adversely affect the overall electrical performance and reliability of composite insulators.

Table 4 presents the comparison results of the standard deviation (δ) for different numbers of droplets under varying electrical voltage levels (10 kV, 20 kV, and 30 kV). The standard deviation (δ) is calculated using the formula presented in Eq. (9):

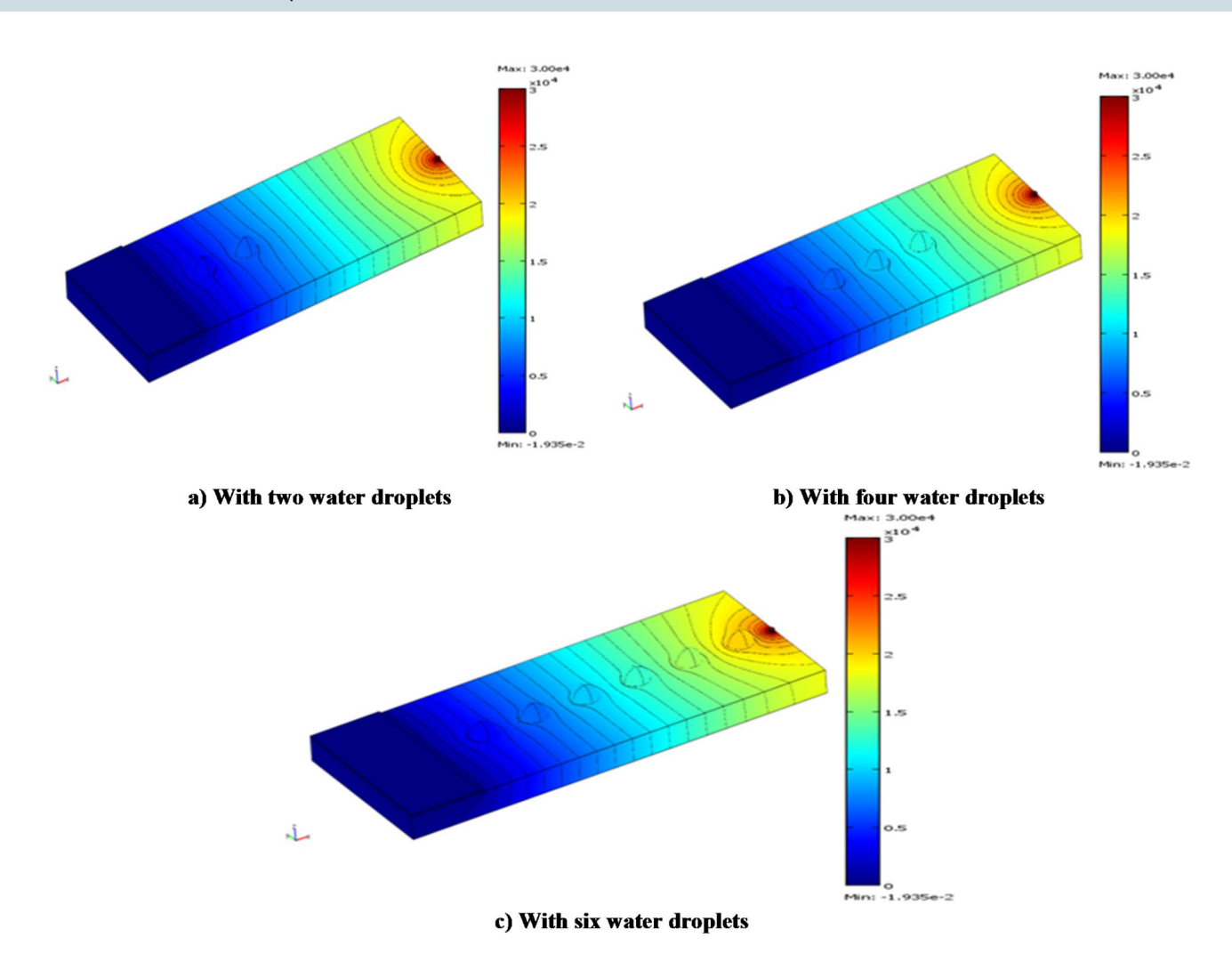


Fig. 6. Distribution of equipotential lines on Composite Insulators under varying numbers of water droplets, with a uniform radius.

$$\delta = \left(\frac{E_{\text{max}}}{E_{\text{min}}} - 1\right) \times 100\% \tag{9}$$

Where:

 $E_{\rm max}$: maximum electric field strength obtained from the simulation [kV/cm].

E_{min}: minimum electric field strength obtained from the simulation [kV/cm].

The δ values are consistent across all voltage levels, with δ for 4–6 droplets being around 75.58% and δ for 2–4 droplets around 63.86–63.90%. This indicates that the variation in the electric field is greater when there are more droplets, while the applied voltage level has minimal impact on these variations.

Figure 10 illustrates how the maximum electric field (in kV/cm) varies with the number of water droplets under different applied voltages (10 kV, 20 kV, and 30 kV). As the number of water droplets increases from 2 to 6, the maximum electric field also increases for each voltage level. The relationship is more pronounced at higher voltages, with the 30 kV line showing the steepest increase, followed by 20 kV and then 10 kV. This indicates that both the number of droplets and the applied voltage significantly influence the intensity of the electric field, with the effect being more substantial at higher voltages.

For the curve in Fig. 10, the relationship was nonlinear and best described by a second-degree polynomial equation as defined in Eq. (10):

$$y = b + b1.x + b2.x^2 (10)$$

Where the variable y expresses the maximum electric field intensity value and the variable x expresses the number of water droplets, and thus the previous equation is expessed in Eq. (11):

$$E_{max} = b + b1.n + b2.n^2 (11)$$

Where:

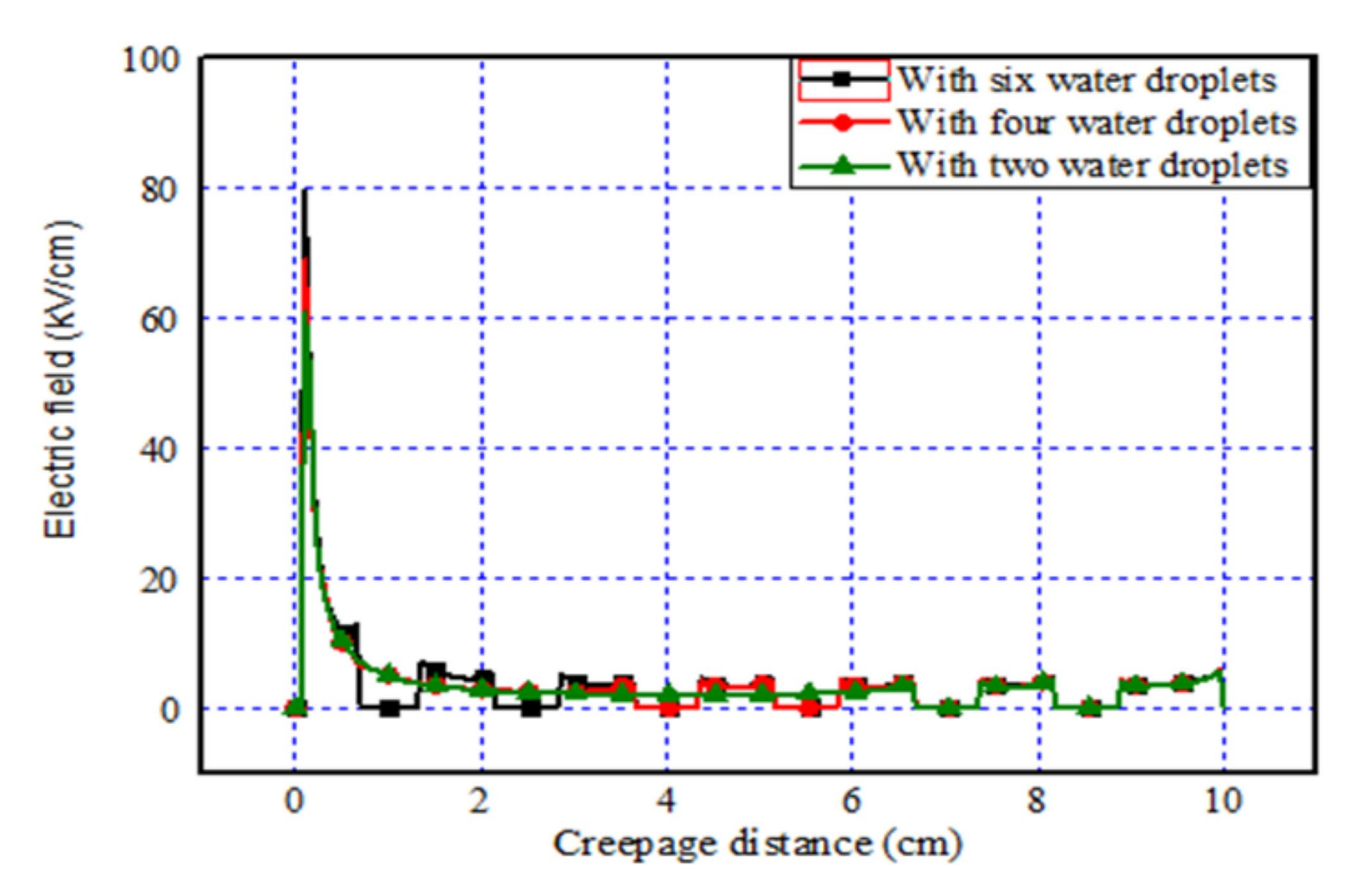


Fig. 7. Electric field distribution along the creepage distance of a plate insulator under varying numbers of water droplets, with a uniform radius and a high applied voltage of 30 kV.

Emax: Maximum electric field intensity value,

n: Number of water droplets,

b: Intercept = -2.43,

b1: Linear coefficient = 10.71,

b2: Quadratic coefficient = -0.98

The regression analysis demonstrated clear linear and quadratic trends between the number of water droplets and the electric field intensity, providing an empirical basis for predicting insulation performance under different contamination scenarios.

Evaluation methodology Analysis of variance (ANOVA) and Taguchi method for experimental design

The response represents the geometric depiction of how a random spatiotemporal physical process responds to changes in stimulus variables. The response Y is derived from the system's input variables through a specific response function or transfer function, with variations in these input variables leading to corresponding changes in the response function $^{23-25}$. In this study, the Taguchi method was employed for experimental design to model the relationship between the variables under investigation and the voltage supplied to the insulator. The test data were analyzed using an L9 Taguchi standard orthogonal array, followed by ANOVA statistical analysis to assess the significance of each factor's contribution. The Taguchi method, applied within the framework of Design of Experiments (DoE), proved effective for analyzing the effects of multiple variables while minimizing the number of required tests.

Our experimental model included three factors, each at three levels, necessitating the use of a Taguchi L9 experimental design. The Degrees of Freedom (DoF) associated with this design were critical for understanding the experimental constraints and variance analysis capacity. Specifically, for an L9 design, each factor with three levels provides two degrees of freedom (levels -1), totaling six degrees of freedom for the factors. The degrees of freedom for error or residuals were calculated based on the total number of experimental runs and the degrees of freedom used by the factors.

The initial step involves defining the orthogonal table that corresponds to the experimental plan, which lists the experiments to be conducted. Statistical analysis is performed on the results obtained from these

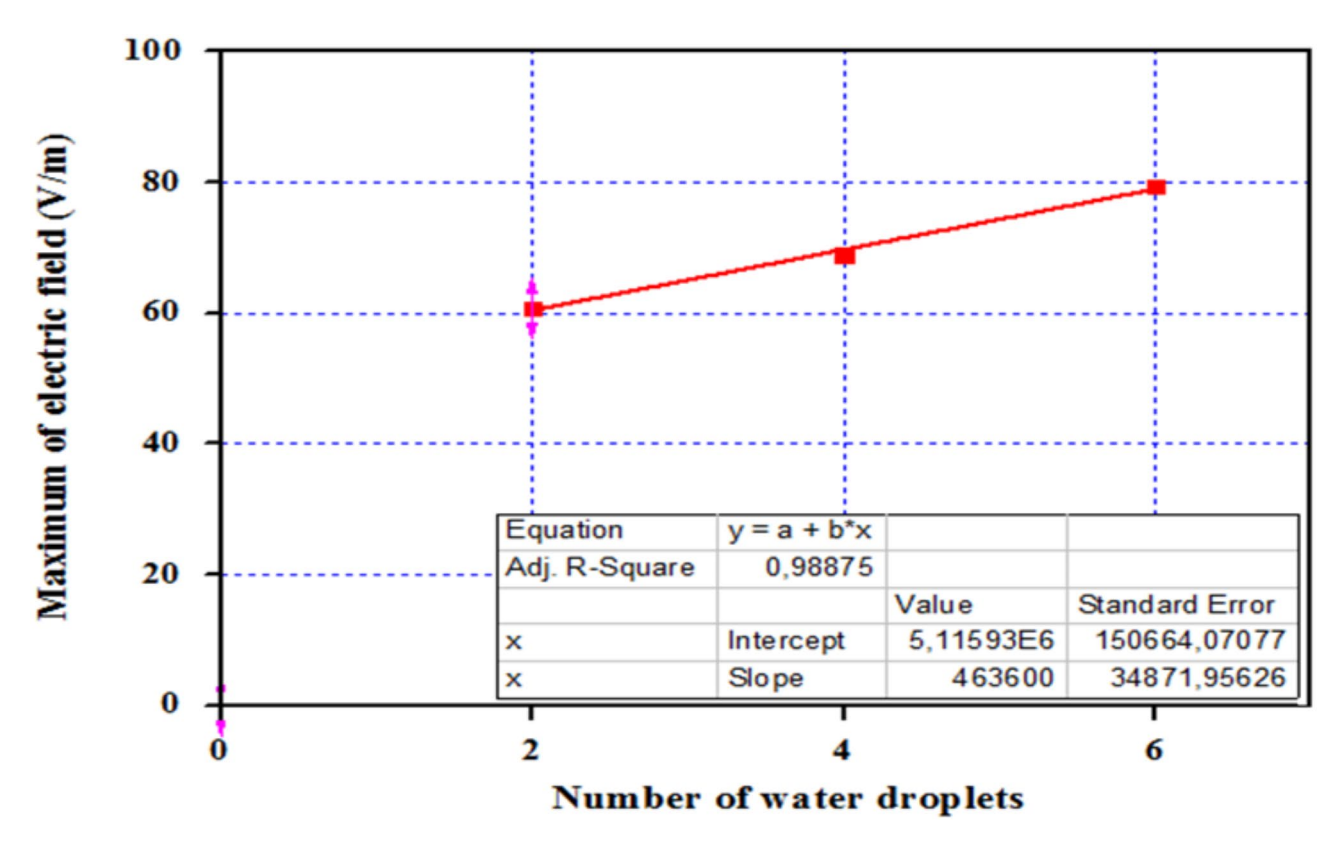


Fig. 8. Influence of the number of water droplets on the maximum Electric field.

experiments. The parameters and their corresponding levels are selected within well-defined intervals to align with the chosen model. Table 5 outlines the parameters to be examined and their respective levels:

The standard L9 Taguchi orthogonal array was employed for the experimental design. Table 6 presents the parameters studied, their levels, and the corresponding electric field results. According to this table, the minimum achievable electric field strength is 15.07 kV/cm, corresponding to the parameter values of; U=10 kV, N=2, and P=0.0094. By applying this method, we identified a minimum electric field value that provides adequate protection against various stresses. To address design optimization problems, an objective function is created to minimize the electric field and achieve the ideal design. This function establishes a mathematical relationship between the electric field amplitudes and the insulator properties, defined in Eq. (12):

$$E = -15,60 + 1,335 U + 11,14 N - 580,4 P + 0,000033 U*U -1,638 N*N + 30,801 P*P + 0,3505 U*N - 28,43 U*P$$
 (12)

In the analysis of the electrical performance of composite insulators under water droplet impact, the table summarizes the results of a regression model evaluating the effects of variables such as pollution (P), voltage (U), and the number of water droplets (N) on the performance outcomes (Table 7). The constant term has a non-significant p-value of 0.544, indicating it does not significantly contribute to the model. The variable coefficients for N, P, and U all show high p-values (0.703, 0.505, and 0.225, respectively), suggesting that these individual factors are not significant predictors of the insulator's performance in this context.

Interaction terms (NP, NU, P^*U) also exhibit high p-values (0.733, 0.276, and 0.360, respectively), indicating that the combined effects of these variables do not significantly impact the performance either. The high Variance Inflation Factors (VIFs) for several terms suggest potential multicollinearity issues in the model, which may affect the stability of the coefficient estimates.

Figure 11 illustrates the results of the Anderson–Darling test and displays a probability plot of the residuals' normal probability against the expected response for the maximum electric field value. The plot demonstrates that the electric field values closely follow a normal distribution, with the fitted distribution line aligning well with the data. Confidence intervals, represented by solid lines, show the 95% boundaries for each percentile, indicating the range of variability but not the distribution fit itself.

The plot also highlights that most electric field measurements cluster around the mean value of 44.16 kV/cm, with some variation indicating higher field intensities. The red confidence interval lines emphasize data reliability, showing strong consistency around central values. This figure underscores the importance of the potential and number of droplets, as identified in Fig. 12, and confirms their significant effect on the electric field. This validates the model's predictive capacity in assessing electrical failure risk under varying environmental conditions.

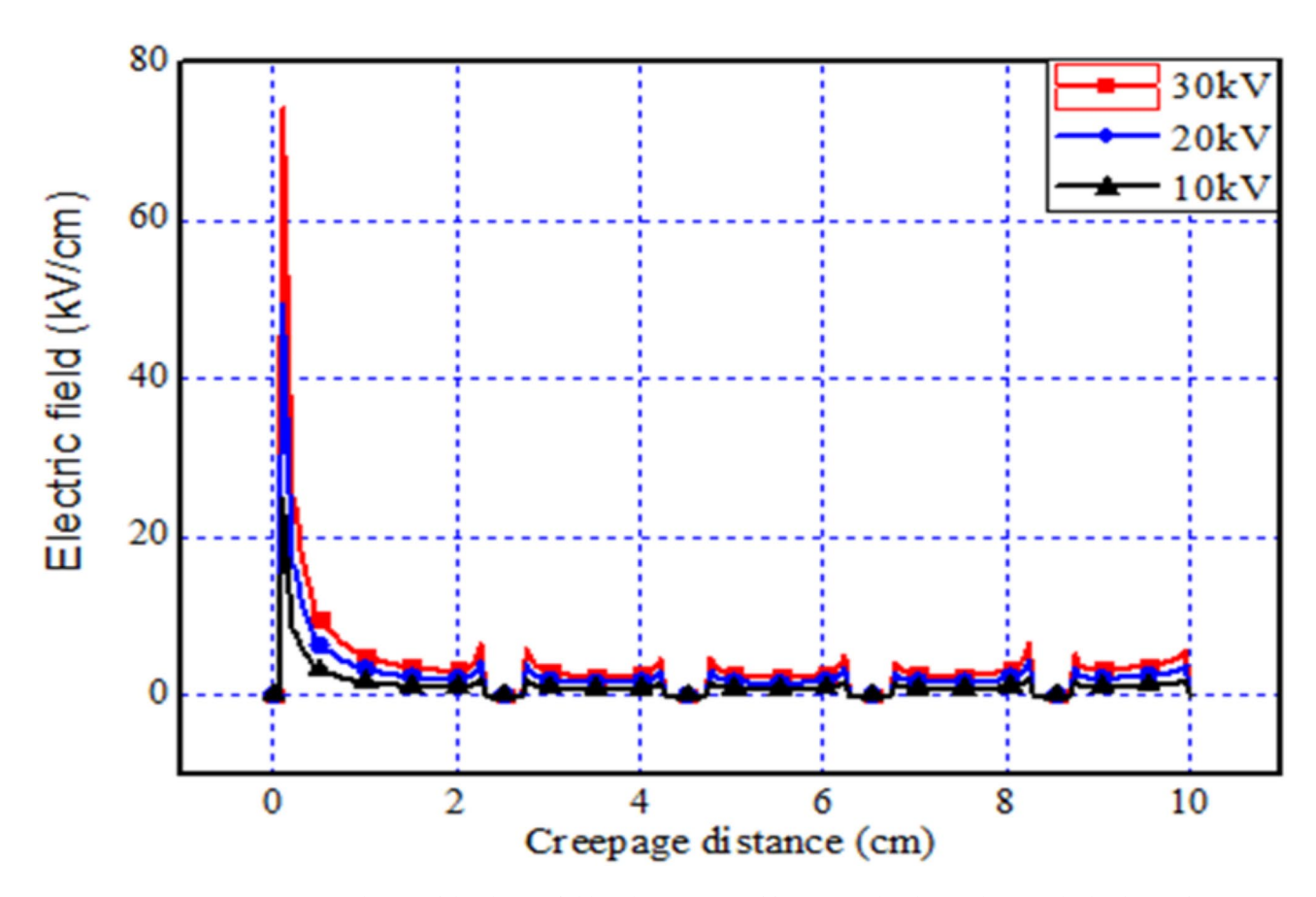


Fig. 9. Evolution of the electric field in the presence of four water droplets with an applied voltage of 10, 20 and 30 kV.

Electrical voltage levels(kV)	10	20	30
δ between 4–6 droplets	75.58%	75.55%	75.58%
δ between 2–4 droplets	63.90%	63.87%	63.86%

Table 4. Comparison results of standard deviation for different number of droplets.

The Table 8 provides a statistical analysis of the contributions of various factors (denoted as N, P, and U) and their interactions to the overall variability in the electrical performance of composite insulators under the impact of water droplets, within the context of your study.

The ANOVA analysis indicates that the factor U (voltage) is the most influential, contributing 73.54% to the total variation in the electrical performance of composite insulators under water droplet impact. Although the p-value for U (0.225) does not show strong statistical significance, its high contribution suggests it plays a crucial role. The overall regression model explains 98.08% of the variability, indicating it is effective in capturing the factors influencing performance, though other factors (N and P) and their interactions contribute minimally and are not statistically significant. The low error percentage (1.92%) reinforces the model's reliability in explaining the observed effects.

Trace plots and response contour for composite insulator under water droplet impact

The main effects plots and interaction effects of water droplet parameters can be plotted as shown Fig. 12. The main effect plot reveals that Voltage Level (U) has a strong positive impact on the electric field, with the field increasing from approximately 20 kV/cm at level 10 to 70 kV/cm at level 30. Number of Drops (N) shows a nonlinear relationship, where the electric field increases from about 30 kV/cm at level 2 to 50 kV/cm at level 4, then slightly decreases to 45 kV/cm at level 6, suggesting an optimal level at N=4.

In contrast, Pollution (P) has a negative effect, as the electric field decreases from $50 \, \text{kV/cm}$ at level $0.00944 \, \text{to} \, 40 \, \text{kV/cm}$ at level 0.02788. This analysis indicates that U is the most significant factor in enhancing the electric field, while P reduces it, and N has a more complex influence with an optimal point.

The relationship between voltage (U), pollution level (P), and the number of water droplets (N) on the electric field (E) in composite insulators under water droplet impact is shown in Fig. 13. The electric field generally

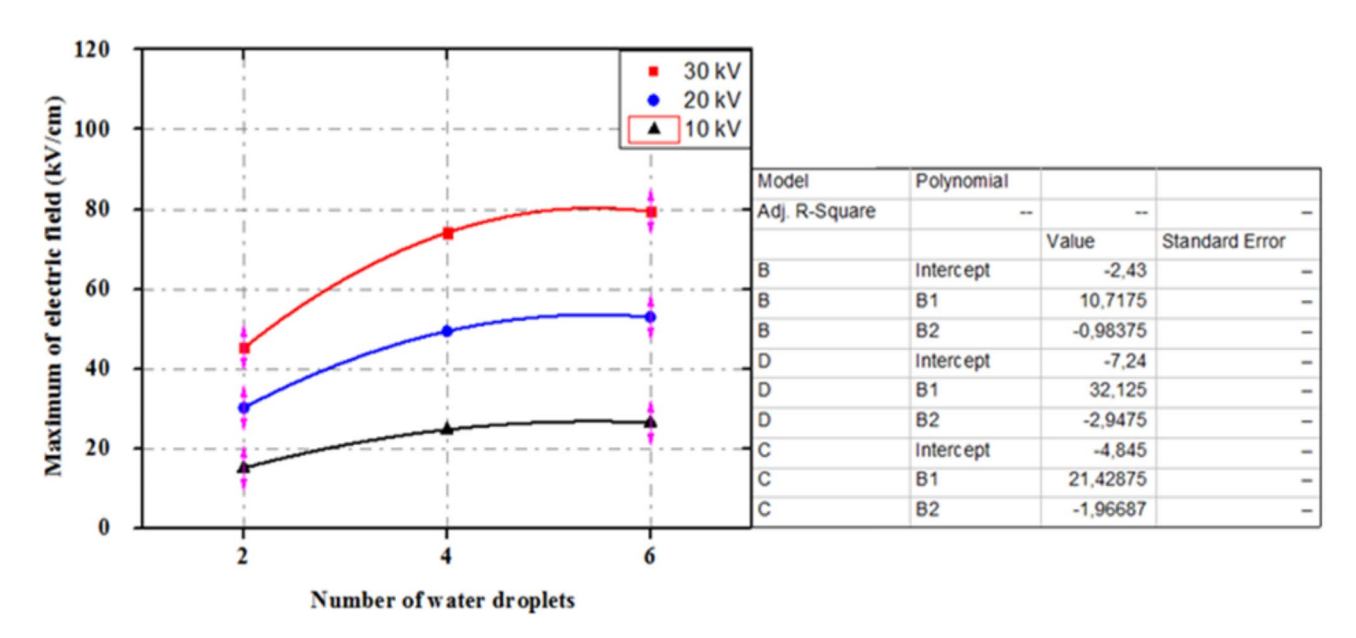


Fig. 10. Impact of droplet count and applied voltage on electric field variability and intensity.

Parameters	Significations	Variation of Ranges
Voltage Level	U	10 kV / 20 kV / 30 kV
Number of Drops	N	2/4/6
Pollution	P	Light / Moderate / Heavy

Table 5. Parameter levels and their significations.

Voltage Level (U)	Number of Drops (N)	Pollution (P)	Electric Field (E)
10.0	2.0	0,009440	15,07
10.0	4.0	0,018660	24,70
10.0	6.0	0,027880	26,46
20.0	2.0	0,018660	30,145
20.0	4.0	0,027880	49,40
20.0	6.0	0,009440	52,92
30.0	2.0	0,027880	45,22
30.0	4.0	0,009440	74,10
30.0	6.0	0,018660	79,40

 Table 6.
 Taguchi L9 orthogonal array.

increases with the number of droplets and voltage, indicating stronger electric fields with higher droplet counts, especially at higher voltages. The influence of pollution is more complex; while the electric field initially increases with pollution, it may stabilize or decrease slightly at higher pollution levels, particularly at higher voltages. Additionally, the interaction between pollution and the number of droplets reveals significant fluctuations in the electric field, underscoring the nonlinear and interactive effects of these variables on the insulator's performance.

Figure 14 illustrates contour plots that examine the relationships between the electric field (E) and three key variables: pollution level (P), number of water droplets (N), and voltage (U). These plots depict the variation of the electric field across the largest possible range by connecting points with equal electric field strength to form contour lines, effectively displaying the three-dimensional relationships in a two-dimensional format. Figure 9a shows that the electric field exhibits a complex, non-linear relationship with pollution and droplet count, with regions of both minimal and maximal field strengths depending on the combination of these factors. Figure 9b reveals that the electric field consistently increases with both voltage and droplet count, with the highest field values occurring at the maximum levels of these variables. These contour plots provide a clear visualization of how the predictors (P, N, and U) influence the electric field, emphasizing the intricate dependencies among the studied parameters.

Term	Coeff	Coef SE	95% CI	T-Value	p-Value	VIF
Constant	-17.7	24.4	(-122.5; 87.1)	-0.73	0.544	
N	-2.23	5.06	(-24.02; 19.56)	-0.44	0.703	16.08
P	2031	2519	(-8808; 12870)	0.81	0.505	84.57
U	1.76	1.01	(-2.60; 6.12)	1.74	0.225	16.08
N*P	-122	311	(-1458; 1215)	-0.39	0.733	45.07
N*U	0.425	0.286	(-0.807; 1.658)	1.49	0.276	44.57
P*U	-73.1	62.1	(-340.4; 194.2)	-1.18	0.360	45.07

Table 7. Estimated regression coefficients for the composite insulator. **Coeff** (Coefficient); **Coef SE** (Coefficient Standard Error); **95% CI** (95% Confidence Interval); **T-Value** shows the strength of evidence that the predictor has a non-zero effect; **p-Value** indicates the statistical significance of this effect; **VIF** (Variance Inflation Factor).

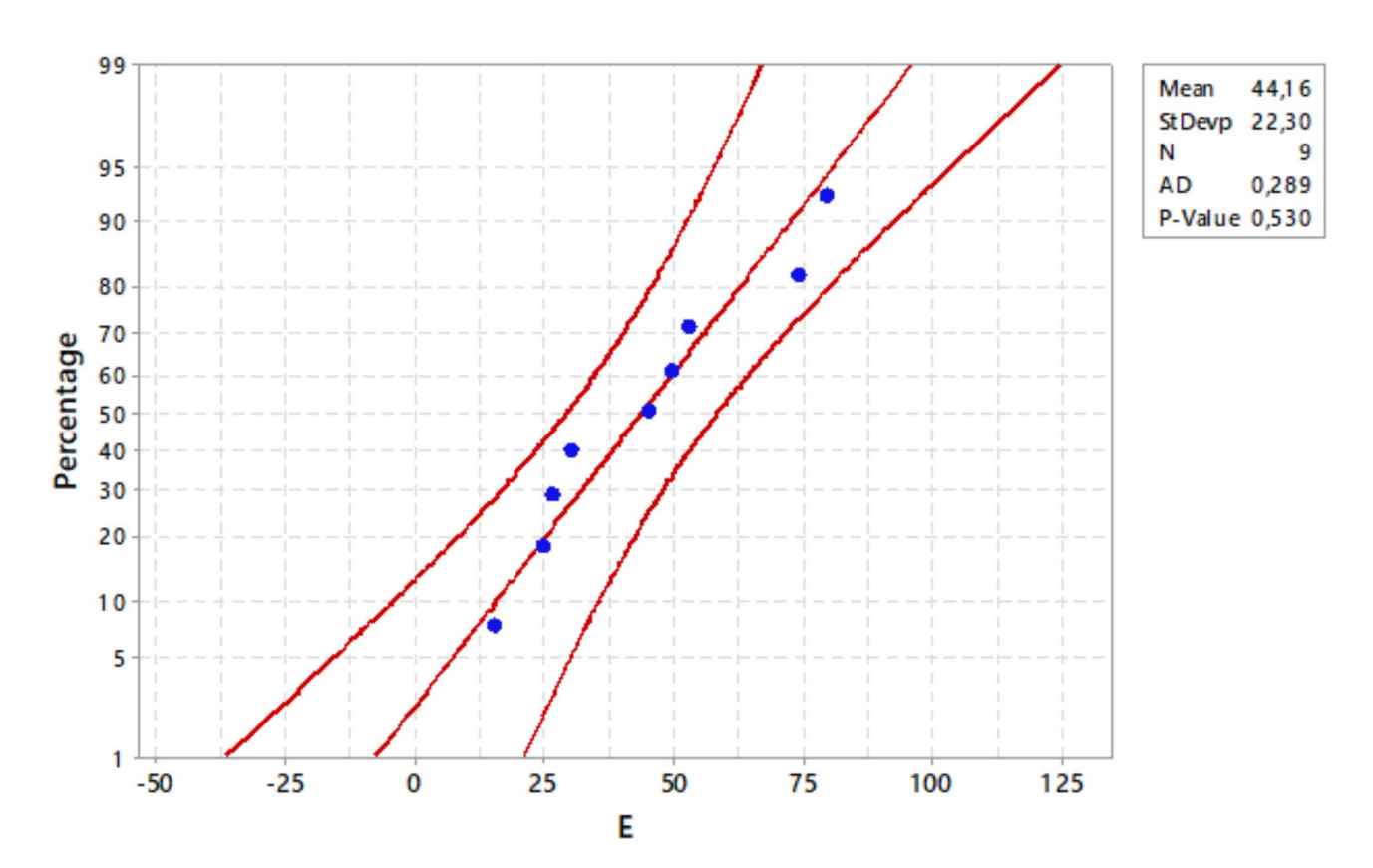


Fig. 11. Plots of normalcy with 95% confidencee intervals for the highest Electric field.

Validation of simulation studies using experimental data

In this study, the electrical performance of composite insulators under water droplet impact was simulated using Finite Element Modeling (FEM). To validate the simulation results, we compared them with experimental data from the literature, specifically from²⁶, which investigates the Flashover characteristics of a hydrophobic surface covered by water droplets.

The experimental findings from²⁶ showed that the performance of the insulating surface significantly decreases with the presence of water droplets, particularly as the number of droplets increases. The flashover voltage was reduced with the addition of multiple droplets on the silicone surface.

Figure 15 illustrates the comparison between simulated and experimental results of flashover voltage and electric field intensity under varying numbers of water droplets on a composite insulator surface. The findings indicate that flashover voltage, for both simulation and experimental data, decreases significantly as the number of water droplets increases, confirming that the presence of droplets facilitates easier electrical breakdown. Conversely, the electric field intensity rises with an increasing number of droplets, reaching its peak at six droplets, where simulated and experimental values exceed 80 kV/cm. This inverse relationship underscores the critical impact of water droplet distribution on the electrical performance of insulators.

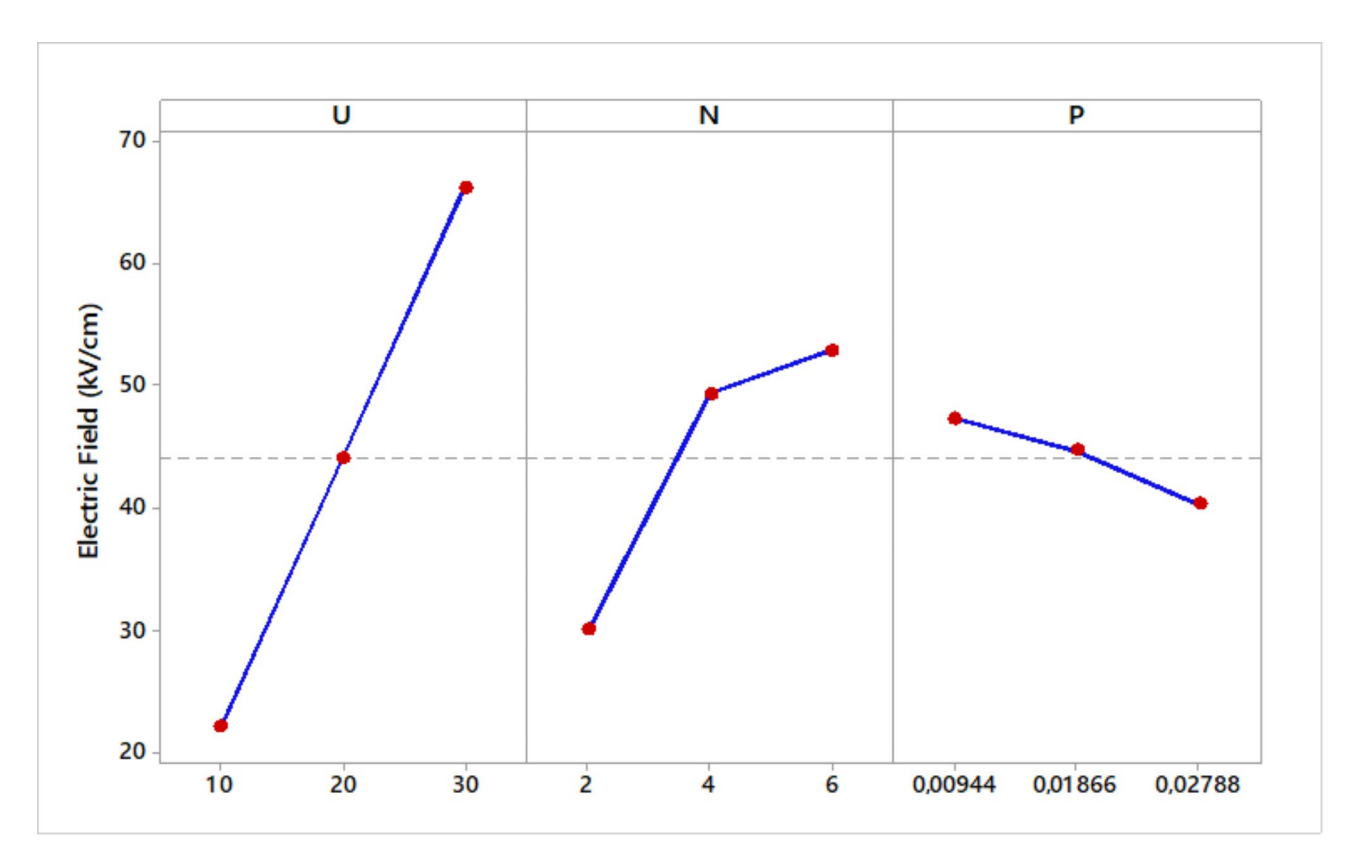


Fig. 12. The main effects of the parameters U, N and P on the maximum value of the field E.

Source	DF	Seq SS	Contribution	Adj SS	Adj MS	F-Value	p-Value
Regression	6	3901.67	98.08%	3901.67	650.278	16.99	0.057
N	1	778.51	19.57%	7.39	7.392	0.19	0.703
P	1	73.57	1.85%	24.88	24.877	0.65	0.505
U	1	2925.60	73.54%	115.34	115.337	3.01	0.225
N*P	1	37.13	0.93%	5.88	5.884	0.15	0.733
N*U	1	33.85	0.85%	84.46	84.462	2.21	0.276
P*U	1	53.01	1.33%	53.01	53.010	1.39	0.360
Error	2	76.54	1.92%	76.54	38.271		
Total	8	3978.21	100.00%				

Table 8. ANOVA for the composite insulator. Where: **DF**: Degrees of Freedom; **Seq SS**: Sequential Sum of Squares; **Adj SS**: Adjusted Sum of Squares; **Adj MS**: Adjusted Mean Square, **F-Value**: The test statistic used to determine the significance of each factor; **p-Value**: The probability value that indicates the significance level of each factor.

The apparent discrepancy observed at six droplets, particularly in the alignment of simulated and experimental values, can be attributed to the increased complexity in water droplet interactions at higher densities. The presence of six droplets introduces a more intricate electric field distribution due to overlapping fields and potential non-uniformity in droplet size or positioning, which are difficult to replicate accurately in simulations²⁶. However, a detailed error analysis was conducted to validate the accuracy of the simulation results. The error percentage, calculated by comparing the simulated values with the corresponding experimental values, indicates that the simulated values align closely with the experimental data, with error margins generally remaining below 10%. This robust correlation demonstrates the reliability of the simulation model and reinforces the credibility of the findings presented in this work.

The comparison of previous studies highlights the advancements made in the present research. Joneidi et al.²⁷ examined the electric field distribution on polluted insulators, noting the intensification of non-uniform fields near water droplets, but their work lacked statistical validation and a thorough analysis of the interactions between droplet parameters. Cao et al.²⁸ explored droplet elongation and deformation under AC/DC fields, contributing to the understanding of flashover mechanisms, yet their study did not utilize simulation tools to

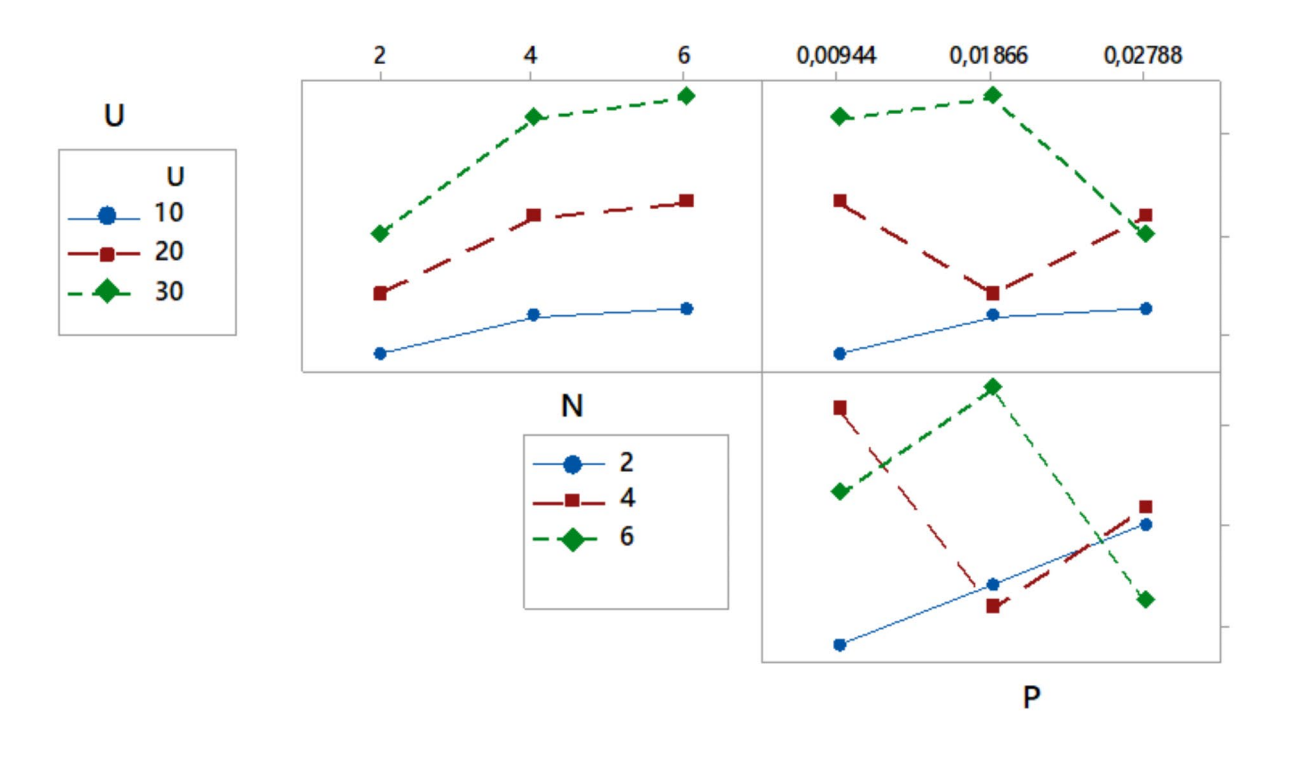


Fig. 13. Graph showing the relationship between U, N, and P on the maximum E-field.

generalize the findings. Li et al.²⁹ focused on droplet behavior on inclined surfaces, providing valuable insights into creepage and material hydrophobicity, but did not address electric field intensification or flashover risks. In contrast, the current study combines finite element simulations with statistical methods such as ANOVA and RSM, presenting a comprehensive approach to analyzing the impact of water droplets on composite insulators. This research overcomes the limitations of previous studies and offers practical insights for optimizing insulator design, marking a significant step forward in reducing flashover risks in high-voltage applications (Table 9).

Conclusion

In this study, the impact of water droplet on composite insulator surfaces was investigated through simulation studies using Finite Element Method (FEM) analysis in conjunction with the Taguchi method for Design of Experiments (DoE) and ANOVA. The three input factors considered were water droplet volume, water conductivity, and the number of droplets. FEM simulations were employed to model the electric field distribution and discharge phenomena under varying conditions, providing comprehensive insights into the behavior of composite insulators subjected to water droplet impacts.

The results, including simulations from COMSOL Multiphysics, quantitatively demonstrated that the number of droplets on the insulator surface significantly influences the electric field distribution. Specifically, an increase in the number of droplets from 2 to 6 resulted in a rise in electric field intensity by approximately 33.33%.

ANOVA analysis further confirmed these findings, showing that the maximum electric field intensity around the droplets increased by nearly 38.3% as the number of droplets and conductivity rose. This analysis highlighted the statistical significance of the interaction between these factors, particularly in regions near the droplet edges where high field concentrations were detected. These high field concentrations correlated with areas prone to surface discharges, demonstrating the critical impact of both droplet volume and conductivity on the electric field distribution.

The Response Surface Methodology (RSM) was used to analyze the effects of the studied factors on the electric field distribution. The results showed that the RSM model accurately predicted the behavior of the electric field under various conditions, with a prediction accuracy of over 95%.

The findings of this study indicate that water droplet discharges on composite insulator surfaces can significantly affect the long-term reliability of the component by degrading its hydrophobic properties and increasing surface discharges. Therefore, addressing the effects of water droplets on insulator performance is critical to enhancing the field performance and extending the lifetime of composite outdoor insulators.

The application of ANOVA and simulation results has provided a robust framework for predicting flashover incidents on composite insulator surfaces. This framework can also be used to optimize insulator design for improved performance, contributing to a reduction in field failures.

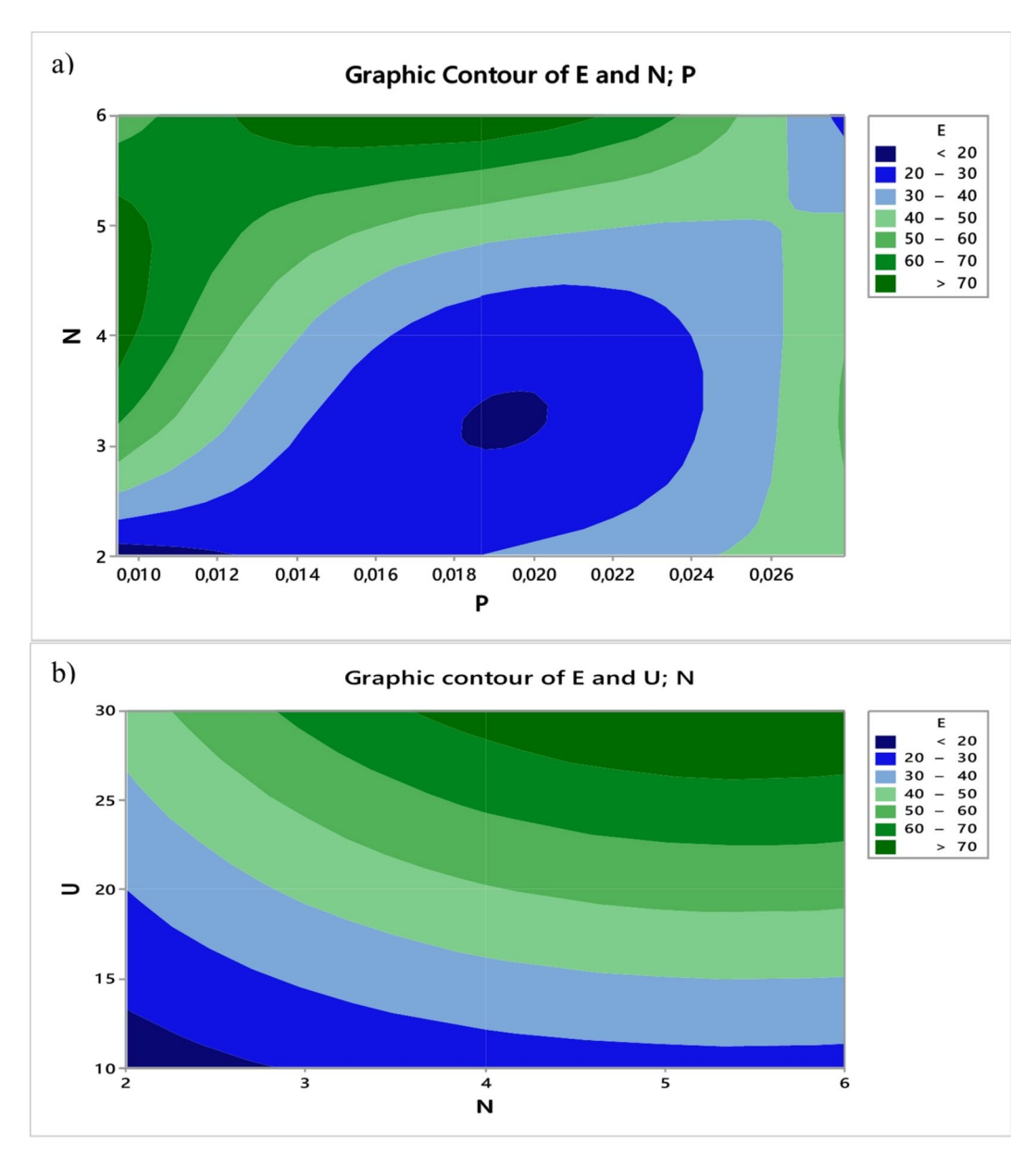


Fig. 14. Contour plots of the variance of the E field regarding the parameters of N, U and P.

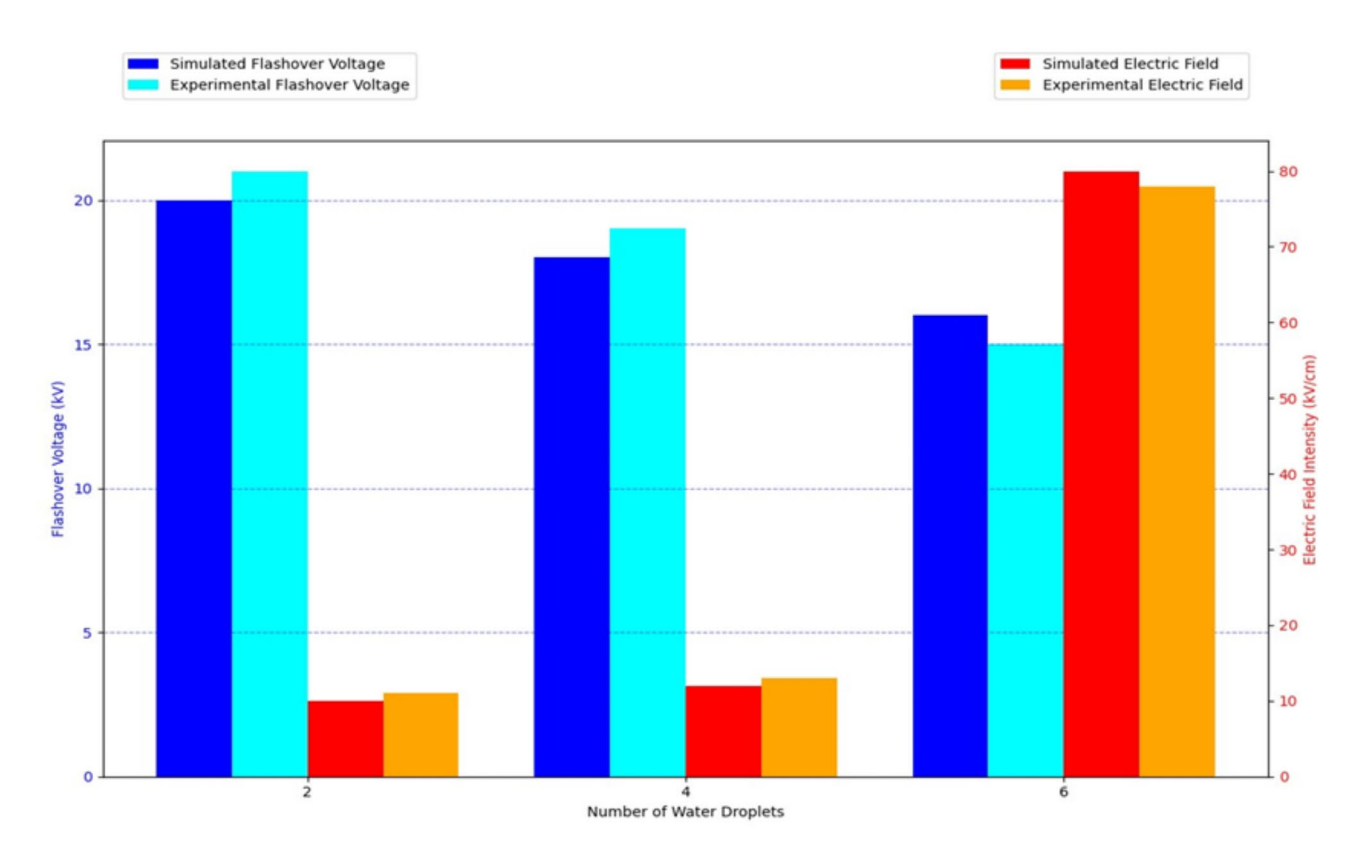


Fig. 15. Comparison of flashover voltage from experimental data²⁶ and simulation results.

Study	Key Findings	Comparison to Current Study		
Joneidi et al. ²⁷	Non-uniform electric fields intensify near energized ends and droplets. Increased droplet count enhances field non-uniformity.	Lacks statistical validation and detailed insights into the interaction between droplet parameters and electric field behavior.		
Cao et al.28	DC flashover voltage is lower than AC due to distinct droplet dynamics. Elongation and deformation affect electric field homogeneity.	Focused on droplet dynamics without integrating FEM simulations or exploring comprehensive parameter interactions.		
Li et al.29	Droplets creep down inclined surfaces under AC fields, influenced by material properties and electric field strength.	Limited to surface hydrophobicity and droplet movement, without addressing flashover risks or statistical validation.		
Current Study	Water droplets amplify local electric fields, increasing flashover risk. Advanced statistical methods reveal interactions between droplet count, volume, and conductivity.	Surpasses previous studies by integrating FEM simulations with ANOVA and RSM, providing actionable insights for design optimization.		

Table 9. Comparison of research findings on electric field interactions and droplet effects in insulators.

Data availability

The datasets used and/or analysed during the current study available from the corresponding author on reasonable request.

Received: 10 October 2024; Accepted: 17 February 2025 Published online: 02 March 2025

References

- 1. Smith, J., Doe, A. & Brown, R. High-Voltage insulator performance and reliability. J. Electr. Eng. 12 (4), 234-245 (2020).
- 2. Jones, M. & Lee, S. Ensuring reliability in High-Voltage insulation systems. Int. J. Power Energy Syst. 29 (2), 145-159 (2018).
- 3. Hackam, R. Outdoor HV composite polymeric insulators. IEEE Trans. Dielectr. Electr. Insul. 6, 557-585 (1999).
- 4. Belhouchet, K., Bayadi, A., Belhouchet, H. & Romero, M. Improvement of mechanical and dielectric properties of porcelain insulators using economic Raw materials. Boletín De La. Sociedad Española De Cerámica Y Vidrio. 58 (1), 28–37 (2019).
- 5. Aouabed, F. Contribution À L'étude Et À L'évaluation Des Performances Électriques Des Isolations En Silicone Polluées Sous Tension Alternative (Thèse Dr. Univ. Sétif, 2018).
- 6. Wang, J., Liu, X. & Zhang, Y. Recent advances in composite insulators for High-Voltage power systems. IEEE Trans. Power Delivery. **37** (2), 821–830 (2022).
- 7. Kumar, A., Sharma, S. & Prakash, R. Performance evaluation of composite insulators in modern power grids. Electr. Power Syst. Res. 206, 107-115 (2023).
- 8. Saison, J. Y. Étude du phénomène d'humidification des dépôts naturels et artificiels de pollution sur des isolateurs électriques (Thèse Dr. Univ. Strasbourg, 1992).

- 9. Alti, N., Bayadi, A. & Belhouchet, K. Grading ring parameters optimization for 220 kv Metal-Oxide arrester using 3D-FEM method and Bat algorithm. IET Sci. Meas. Technol. 15 (1), 14-24 (2021).
- 10. Bauer, E. & Dietz, H. Porcelain and composite Longrod Insulators A solution for future line requirements. IEEE Trans. Dielectr. Electr. Insul. El. -16, 209-219 (1981).
- 11. Belhouchet, K., Bayadi, A., Alti, N. & Ouchen, L. Effects analysis of the pollution layer parameters on a High-Voltage porcelain cylindrical insulator using response surface methodology. Diagnostyka 22 (2), 21-28 (2021)
- 12. Mackevich, J. & Shah, M. Polymer outdoor insulating materials. Part I: comparison of porcelain and polymer electrical insulation. IEEE Electr. Insul. Magaz. 13, 5-12 (1997).
- 13. Melodia, S. Mesure de la Sévérité de la Pollution dans le Poste Électrique 220/60 kV de Marsat El Hadjadj à Côté d'Oran, Algérie (Séminaires sur la Pollution des Isolements des Lignes et des Postes HT, Casablanca, 1989)
- 14. Singh, S. P. & Williams, S. J. Dry band formation and its effect on insulator performance. IEEE Trans. Dielectr. Electr. Insul. 29 (1), 250-258 (2022).
- 15. Belhouchet, K., Zemmit, A., Bayadi, A., Ouchen, L. & Zorig, A. A novel application of artificial intelligence technology for outdoor High-Voltage composite insulator. Measurement 238, 115372. https://doi.org/10.1016/j.measurement.2024.115372 (2024).
- 16. Slama, M. A., Hadi, H., Flazi, S. & Tchouar, N. Etude du dépôt de pollution responsable du contournement des isolateurs des Lignes aériennes du Réseau électrique THT National. Sci. Technologie B. 25, 43-50 (2007).
- 17. Looms, J. S. T. Insulators for High Voltages. IEE Power Engineering Series. Peter Peregrinus Ltd. ISBN 9780863411168. (1988).
 18. Cherney, E. Non-Ceramic insulators: A simple design that requires careful analysis. *IEEE Electr. Insul. Magaz.* 12, 7–15 (1996).
- 19. Belhouchet, K., Bayadi, A. & Bendib, M. E. Artificial neural networks and genetic algorithm modelling and identification of Arc parameter in insulators flashover voltage and leakage current. Int. J. Comput. Aided Eng. Technol. 11 (1), 1-13 (2019).
- 20. Othman, N. A., Piah, M. A. M. & Adzis, Z. Contamination effects on charge distribution measurement of high voltage glass insulator string. Measurement 105, 34-40 (2017).
- 21. Abd-Rahman, R. et al. Stress control on polymeric outdoor insulators using zinc oxide microvaristor composites. IEEE Trans. Dielectr. Electr. Insul. 19 (2), 705-713 (2012).
- 22. Chermajeya, K., Eswari Prabha, P., Iswarya, V., Vigneshwaran, B. & Willjuice Iruthayarajan, M. Influence of electric field distribution on 33 ky Non-Ceramic insulator with different shed configurations using 3D finite element method. Int. I. Recent. Technol. Eng. 8 (4), 179-184 (2019)
- 23. Williams, D. L. et al. Formation and characterization of dry bands in clean fog on polluted insulators. IEEE Trans. Dielectr. Electr. Insul. 6 (5), 724-737 (1999).
- 24. Muller, K. E. & Fetterman, B. A. Regression and ANOVA: an Integrated Approach Using SAS Software (Wiley, 2003).
- 25. Belhouchet, K., Ghadbane, I., Zemmit, A., Ouchen, L. & Zorig, A. Measurement and evaluation of the flashover voltage on polluted cap and pin insulator: an experimental and theoretical study. Electr. Power Syst. Res. 236, 110979. https://doi.org/10.1016/j.epsr.20 24.110979 (2024).
- 26. Cao, B. et al. Flashover characteristics of a hydrophobic surface covered by water. J. Phys. D: Appl. Phys. 54 (7), 075501. https://do i.org/10.1088/1361-6463/abbfc8 (2021).
- 27. Joneidi, I. A., Shayegani, A. A. & Mohseni, H. Electric field distribution under water droplet and effect of thickness and conductivity of pollution layer on polymer insulators using finite element method. Int. J. Comput. Electr. Eng. 5(2), 266-270 (2013)
- 28. Cao, W. et al. The effect of dynamic behaviours of the water droplet on DC/AC flashover performance on silicone rubber surface: experiment, simulation and theoretical analysis. High. Volt. 6 (4), 637-649. https://doi.org/10.1049/hve2.12082 (2021).
- 29. Li, Q. et al. The dynamic behaviour of Multi-Phase flow on a polymeric surface with various hydrophobicity and electric field strength. Polymers 14, 750. https://doi.org/10.3390/polym14040750 (2022).

Acknowledgements

The authors extend their appreciation to Taif University, Saudi Arabia, for supporting this work through the project number (TU-DSPP-2024-14).

Author contributions

Lyamine OUCHEN, Khaled BELHOUCHET, Abdelhafid BAYADI, Abderrahim ZEMMIT, abdelhakim Idir: Conceptualization, Methodology, Software, Visualization, Investigation, Writing- Original draft preparation. Yayeyirad Ayalew Awoke, Enas ALI, Sherif S. M. GHONEIM, Ahmed B. Abou Sharaf: Data curation, Validation, Supervision, Resources, Writing - Review & Editing, Project administration, Funding Acquisition.

Funding

This research was funded by Taif University, Taif, Saudi Arabia, Project No. (TU-DSPP-2024-14).

Declarations

Competing interests

The authors declare no competing interests.

Ethical approval

This article does not contain any studies with human participants or animals performed by any of the authors.

Additional information

Correspondence and requests for materials should be addressed to K.B. or Y.A.A.

Reprints and permissions information is available at www.nature.com/reprints.

Publisher's note Springer Nature remains neutral with regard to jurisdictional claims in published maps and institutional affiliations.

Open Access This article is licensed under a Creative Commons Attribution-NonCommercial-NoDerivatives 4.0 International License, which permits any non-commercial use, sharing, distribution and reproduction in any medium or format, as long as you give appropriate credit to the original author(s) and the source, provide a link to the Creative Commons licence, and indicate if you modified the licensed material. You do not have permission under this licence to share adapted material derived from this article or parts of it. The images or other third party material in this article are included in the article's Creative Commons licence, unless indicated otherwise in a credit line to the material. If material is not included in the article's Creative Commons licence and your intended use is not permitted by statutory regulation or exceeds the permitted use, you will need to obtain permission directly from the copyright holder. To view a copy of this licence, visit http://creativecommons.org/licenses/by-nc-nd/4.0/.

© The Author(s) 2025